Analytic modelling of tidal effects in the relativistic inspiral of binary neutron stars

Luca Baiotti,[1,2] Thibault Damour,[3,4] Bruno Giacomazzo,[5,6,7] Alessandro Nagar,[3] and Luciano Rezzolla[7,8]

[1]*Institute of Laser Engineering, Osaka University, Suita, Japan*
[2]*Yukawa Institute for Theoretical Physics, Kyoto University, Kyoto, Japan*
[3]*Institut des Hautes Etudes Scientifiques, Bures-sur-Yvette, France*
[4]*ICRANet, Pescara, Italy*
[5]*Department of Astronomy, University of Maryland, College Park, MD USA*
[6]*Gravitational Astrophysics Laboratory, NASA Goddard Space Flight Center, Greenbelt, MD USA*
[7]*Max-Planck-Institut für Gravitationsphysik, Albert-Einstein-Institut, Potsdam, Germany*
[8]*Department of Physics and Astronomy, Louisiana State University, Baton Rouge, LA, USA*

To detect the gravitational-wave signal from binary neutron stars and extract information about the equation of state of matter at nuclear density, it is necessary to match the signal with a bank of accurate templates. We have performed the longest (to date) general-relativistic simulations of binary neutron stars with different compactnesses and used them to constrain a tidal extension of the effective-one-body model so that it reproduces the numerical waveforms accurately and essentially up to the merger. The typical errors in the phase over the $\simeq 22$ gravitational-wave cycles are $\Delta\phi \simeq \pm 0.24$ rad, thus with relative phase errors $\Delta\phi/\phi \simeq 0.2\%$. We also show that with a single choice of parameters, the effective-one-body approach is able to reproduce all of the numerically-computed phase evolutions, in contrast with what found when adopting a tidally corrected post-Newtonian Taylor-T4 expansion.

PACS numbers: 04.25.dk, 04.25.Nx, 04.30.Db, 04.40.Dg, 95.30.Sf, 97.60.Jd

Introduction. Inspiralling binary neutron stars (BNSs) are among the strongest sources of gravitational waves (GWs) and certain targets for the advanced and new-generation ground-based GW detectors LIGO/Virgo/GEO/ET [1]. These detectors will be sensitive to the inspiral GW signal up to GW frequencies ~ 1000 Hz, which are reached soon before the merger. The late inspiral signal will be influenced by tidal interaction between the two neutron stars (NSs), which, in turn, encodes important information about the equation of state (EOS) of matter at nuclear densities. However, to reliably extract such information, both a large sample of numerical simulations and an analytical model of inspiralling BNSs which is able to reproduce them accurately, are needed. In this work we report on significant progress on this problem by presenting the longest (to date) simulations of merging equal-mass BNSs and by showing how to use them to calibrate an effective-one-body (EOB) model of tidally interacting BNSs.

Numerical simulations of merging BNSs in full general relativity have a long history (see the Introduction of [2] for a brief review). However, it has been possible only recently to obtain a more precise and robust description of this process and to include additional physical ingredients such as magnetic fields and realistic EOSs. In particular the use of adaptive mesh refinement techniques has made it possible not only to increase the level of accuracy, but also to compute the full evolution of the hypermassive NS up to black hole formation [2, 3], with and without magnetic fields [4], with idealized and realistic cold EOSs [5]. On the other hand, the analytical description of tidally-interacting binary systems has been initiated only very recently [6, 7]. Two major results can be summarized from this bulk of work. First, the dimensionless quantity k_ℓ (Love number) in the (gravito-electric) tidal polarizability parameter $G\mu_\ell \equiv 2k_\ell R^{2\ell+1}/(2\ell-1)!!$ measuring the relativistic coupling (of multipolar order ℓ) between a NS of radius R and the external gravitational field in which it is embedded has been found to be a strongly decreasing function of the compactness parameter $\mathcal{C} \equiv GM/(c^2R)$ of the NS. Second, a comparison between the numerical computation of the binding energy of quasi-equilibrium circular sequences of BNSs [8] and the EOB description of tidal effects [7] has suggested that higher-order post-Newtonian (PN) corrections to tidal effects increase by a factor of order two the tidal polarizability of close NSs. The main aim of this paper is extend the domain of applicability of the EOB method [9], from the inspiralling binary black hole (BBH) case (for which it recently provided a very accurate analytic description [10, 11]), to the yet unexplored case of inspiralling BNSs. To this aim we have performed accurate and long-term BNS simulations covering $\sim 20-22$ GW cycles of late inspiral, and we will show that they can be reproduced accurately almost up to the merger by a new tidal extension of the EOB model, which yields relative phase errors $\Delta\phi/\phi \simeq 0.2\%$.

Tidal corrections in the EOB approach. We recall that the EOB formalism [9] replaces the PN-expanded two-body dynamics by a *resummed* description with, in particular, an Hamiltonian of the form: $H_{\rm EOB} \equiv Mc^2\sqrt{1+2\nu(\hat{H}_{\rm eff}-1)}$, where $M \equiv M_A+M_B$ is the total mass and where $\nu \equiv M_A\,M_B/(M_A+M_B)^2$ is the symmetric mass ratio. Here the "effective Hamiltonian" $\hat{H}_{\rm eff}$ is a simple function of the momenta and it incorporates the relativistic gravitational attraction mainly through the so-called "EOB radial potential" $A(r)$. The structure of $A(r)$ is remarkably simple at 3 PN: $A^{\rm 3PN}(r) = 1-2u+2\,\nu\,u^3+a_4\,\nu\,u^4$, where $a_4 = 94/3-(41/32)\pi^2$, and $u \equiv GM/(c^2 r_{AB})$. An excellent description of BBHs has been found to be given by [10]

$$A^0(r) = P^1_5\left[1-2u+2\nu u^3+a_4\nu u^4+a_5\nu u^5+a_6\nu u^6\right],$$

where P^n_m denotes an (n,m) Padé approximant and where values of the coefficient $a_5 = -6.37$, $a_6 = +50$ provide a very good agreement between EOB and numerical-relativity (NR) waveforms for BBHs [10] (The results presented here are insensitive to this choice as long as a_5, a_6 are chosen in a well defined range). Ref. [7] suggested to include tidal effects as a correction $A^{\rm tidal}(u)$ to the radial potential, *i.e.* $A(u) = A^0(u) + A^{\rm tidal}(u)$, with

$$A^{\rm tidal} = \sum_{\ell \geq 2} -\kappa^T_\ell u^{2\ell+2} \hat{A}^{\rm tidal}_\ell(u)\,. \tag{1}$$

Here $\kappa^T_\ell u^{2\ell+2}$ describes the leading-order (LO) tidal interactions. It is a function of the two masses, of the two compactnesses $\mathcal{C}_{A,B}$, and of the two (relativistic) Love numbers $k^{A,B}_\ell$

$$\kappa^T_\ell \;=\; 2\frac{M_B\, M_A^{2\ell}}{(M_A+M_B)^{2\ell+1}} \frac{k^A_\ell}{\mathcal{C}_A^{2\ell+1}} + \{\, _A \;\leftrightarrow\; _B\}\,. \tag{2}$$

The additional factor $\hat{A}^{\rm tidal}_\ell(u)$ in Eq. (1) represents the effect of higher-order relativistic contributions to the tidal interactions: next-to-leading order (NLO), and next-to-next-to-leading order (NNLO), etc. A number of different prescriptions can be considered for the tidal potential $\hat{A}^{\rm tidal}_\ell$ and these will be presented in a longer companion work [12]. Here, we will limit ourselves to a "Taylor-expanded" expression $\hat{A}^{\rm tidal}_\ell(u) \equiv 1 + \bar{\alpha}^{(\ell)}_1 u + \bar{\alpha}^{(\ell)}_2 u^2$ [7], where $\bar{\alpha}^{(\ell)}_n$ are pure numbers in the equal-mass case, but functions of M_A, $\mathcal{C}_A$ and k^A_ℓ in the general case. The unknown coefficients $\bar{\alpha}_1, \bar{\alpha}_2$ will be constrained via comparison with the simulations. Analogous coefficients parametrizing higher-order relativistic contributions in the waveform, have been found to have a small effect [12] and will be neglected here. Of course, tidal effects can also be accounted for via modifications of one of the *non-resummed* PN description, such as the Taylor-T4 expansion [6]; a comparison between the NR results and the EOB and PN descriptions will be presented below.

In order to measure the influence of tidal effects, it is useful to consider the "phase acceleration" $\dot{\omega} \equiv d\,\omega/dt \equiv d^2\phi/dt^2$, where $\phi \equiv \phi_{22}$ is the phase of either the curvature or of the metric GWs. The function $\dot{\omega}(\omega)$ is independent of the two "shift ambiguities" that affect the GW phase $\phi(t)$, namely the shifts in time and phase, and thus a useful intrinsic measure of the quality of the waveform [14]. Here, however, we use another dimensionless diagnostic to measure the phase acceleration, *i.e.* the phase evolution "quality-factor"

$$Q_\omega(\omega) = \frac{d\phi}{d\,\ln\,\omega} = \frac{\omega\, d\phi/dt}{d\omega/dt} = \frac{\omega^2}{\dot{\omega}}\,. \tag{3}$$

In analogy with the "quality factor" Q of a damped oscillator, $Q_\omega(\omega)$ measures the number of GW cycles spent by the binary within an octave of the GW frequency ω.

Numerical Simulations. They were performed with the `Cactus-Carpet-Whisky` [15] codes and, in essence, we use the same gauges and numerical methods already discussed in [2], to which we refer the reader for details. As initial data we use quasi-equilibrium irrotational binaries generated with the multi-domain spectral-method code `LORENE`, within a conformally-flat spacetime metric [16]. The EOS of the initial data is the polytropic one $p = K\,\rho^\Gamma$, where p, ρ, $K = 123.6$, and $\Gamma = 2$ are the pressure, rest-mass density, the polytropic constant and adiabatic index, respectively (in units where $c = G = M_\odot = 1$). The evolutions are instead performed with either a polytropic EOS or an "ideal-fluid" one, $p = \rho\epsilon(\Gamma - 1)$, where ϵ is the specific internal energy; the differences introduced by the different EOSs are below the numerical error bars and will be detailed in [12]. Because the stellar compactness represents the most important parameter determining the size of tidal effects, we have considered two different binaries having total ADM/baryonic mass of either $2.69/2.89\,M_\odot$ or $3.00/3.25\,M_\odot$, thus with compactnesses $\mathcal{C} = 0.12$ or $\mathcal{C} = 0.14$. Hereafter the two binaries will be referred to as `M2.9C.12` and `M3.2C.14`, respectively. The number of refinement levels and their resolutions are the same as those in [2], but the initial coordinate separation between the stellar centers is of 60 km, considerably larger than the one considered in [2]. This yields about 10 orbits before merger, thus the longest BNS waveforms produced to date.

Discussion. We start our comparison between the NR results and the analytic-relativity (AR) ones by showing in Fig. 1 the Q_ω diagnostics for various possible LO/NLO tidal models and for GW frequencies $M\omega \lesssim 0.06$ (*i.e.* up to $3/5$ GW cycles before merger for the binary `M2.9C.12`/`M3.2C.14`, respectively). The first thing to note is that the EOB LO corrections (dot-dashed line) are clearly insufficient, both for the `M2.9C.12` (upper panel) and the `M3.2C.14` binaries (lower panel), to match the corresponding NR curve (dashed line with open circles). This clearly indicates the need for NLO effects. The dephasing accumulated by EOB LO relative to the NR data over the frequency interval where the simulations overlap is ~ 5 rad, thus much larger than the NR phasing error related to the finite resolution, which was measured to be $\Delta\phi = \pm 0.24$ [12]. By contrast, after suitably choosing the parameters $\bar{\alpha}_1$, $\bar{\alpha}_2$, it is possible to obtain a very good match between the Q_ω curves (solid and dashed lines) and the NR data (dashed line with open circles) for *both* binaries, with a final phase difference that is $\ll 1$ rad.

Several remarks are worth making at this point. First, because of its definition, even fractionally small differences $\Delta Q_\omega \sim 1$ in $Q_\omega \sim 100$ lead to very significant differences (of ~ 1 rad) in the accumulated phases. Second, because it involves several

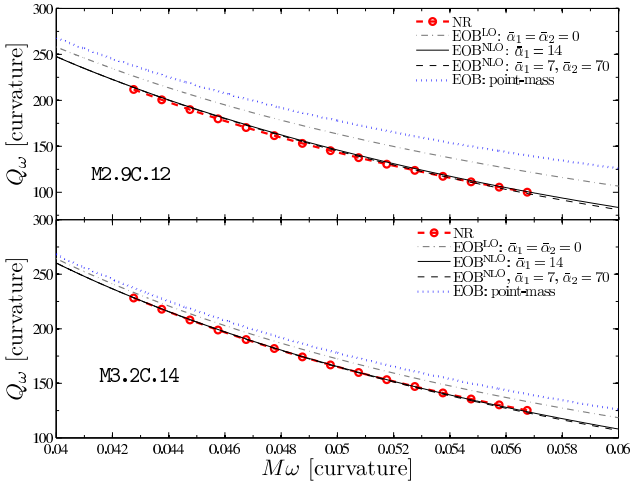

FIG. 1: Comparison of the AR curves for Q_ω at NLO for different choices of the parameters (solid, dashed lines) with the corresponding NR ones (dashed lines with open circles) for the two binaries considered. Also shown are the Q_ω curves for the LO term (dot-dashed line) and when tidal effects are ignored (dotted line).

time derivatives, the calculation of Q_ω is challenging when made from the early-inspiral part of the NR waveforms, as the latter is affected by a series of contaminating errors. These, however, can be filtered out by fitting the NR phase evolution with an analytical expression that reproduces at lower order the behavior expected from the PN approximation (more details will be presented in [12]). Third, all the NLO models are "degenerate" in that several choices of the free parameters can be made that match the NR data with an uncertainty on Q_ω of order 1. Finally, a similarly good agreement can also be obtained with a constant "effective" value of $\hat{A}_\ell^{\rm tidal}(u)$, namely with $k_\ell^{\rm eff}=2.5k_\ell$, which is the same for the two binaries (*cf.* dot-dashed line in Fig. 2). The value of the amplification factor is sensitive to the numerical truncation error and a slightly smaller value (namely ≈ 1.85) is obtained when considering the resolution-extrapolated GWs [12]; this smaller value is also compatible with the estimates suggested by the analysis using the binding energy of circular BNSs [8].

Figure 2 also reports the phase quality-factor as obtained when using the Taylor-T4 approximant either at LO (thick dashed line) or at NLO with different amplification factors (solid and dashed lines). While the introduction of NLO terms does improve the match between the NR data and the Taylor-T4 approximant, the amplification factors are different for the two binaries, with the accumulated dephasing for the `M2.9C.12` binary being about ten times larger than that for `M3.2C.14` for the same amplification factor. In contrast, the EOB amplification factor is equally good for the two binaries, with a dephasing within the numerical error bar. These results suggest that the EOB modelling of LO/NLO tidal effects may be more robust than the corresponding Taylor-T4 one.

We next consider the comparison of the waveforms, in the time domain and *over the full inspiral up to the merger*. This is shown in Fig. 3, whose left panels refer to the `M2.9C.12` binary and the right ones to `M3.2C.14`, and where the top parts compare the (real part) of the EOB and NR metric h_{22} waveform with $\bar{\alpha}_1=7$, $\bar{\alpha}_2=70$, while the bottom panels show the corresponding phase differences, $\Delta\phi^{\rm EOBNR}(t)\equiv\phi^{\rm EOB}(t)-\phi^{\rm NR}(t)$ (suitably shifted in time and phase à la [13]). The two vertical lines indicate two possible markers of the "time of the merger"; more specifically, the dashed lines refer to the time at which the modulus of the metric NR waveform reaches its first maximum, while the vertical dash-dotted line represents the EOB estimate of the "formal" contact [7]. Fig. 3 clearly shows that the agreement in the time domain between the analytic EOB description and the numerical one is extremely good essentially up to the merger, with a phase error which is well within the estimated error bar. Again, a few notes should be made. First, the match between the two descriptions during most of the long inspiral phase is excellent and it is only during the last $100M$ before contact that the dephasing grows significantly. Second, the break-down of the analytic description near the merger is clearly expected and is exaggerated by having chosen as end of the inspiral the maximum of the GW amplitude. Last and most important, once a *single* choice is made for the tidal parameters within the EOB approach, the match is very good for *both* binaries. This is not the case for the Taylor-T4 approximation, for which two different choices are needed to reach a match with the NR waveforms which is also less good than the EOB one.

Conclusions. We have presented the first NR-AR comparison of the GWs emitted during the inspiral of relativistic BNSs. In particular, we have analyzed the longest to date numerical simulations of equal-mass and irrotational BNSs with two different compactnesses. In this way we were able to highlight that tidal effects are significantly amplified by higher-order relativistic corrections even in the early inspiral phase and that NLO corrections are therefore necessary. The present accuracy of the NR data and the incomplete knowledge of the NLO terms leave us with an uncertainty about their functional form and with a number of different choices which currently reproduce the NR data equally well. Nevertheless, when a *single* choice for the free

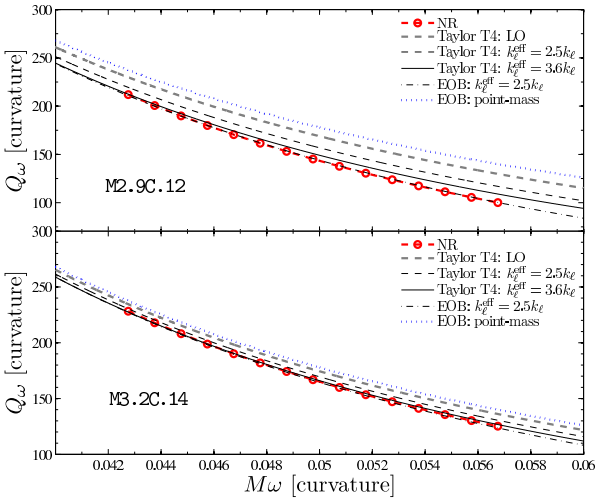

FIG. 2: The same as Fig. 1 but when using the Taylor-T4 approximant either at LO (thick dashed line) or at NLO with different amplification factors (solid and dashed lines). Also shown as a reference is the EOB Q_ω curve at NLO with $\kappa_\ell^{\rm eff} = 2.5\kappa_\ell$ (dot-dashed line).

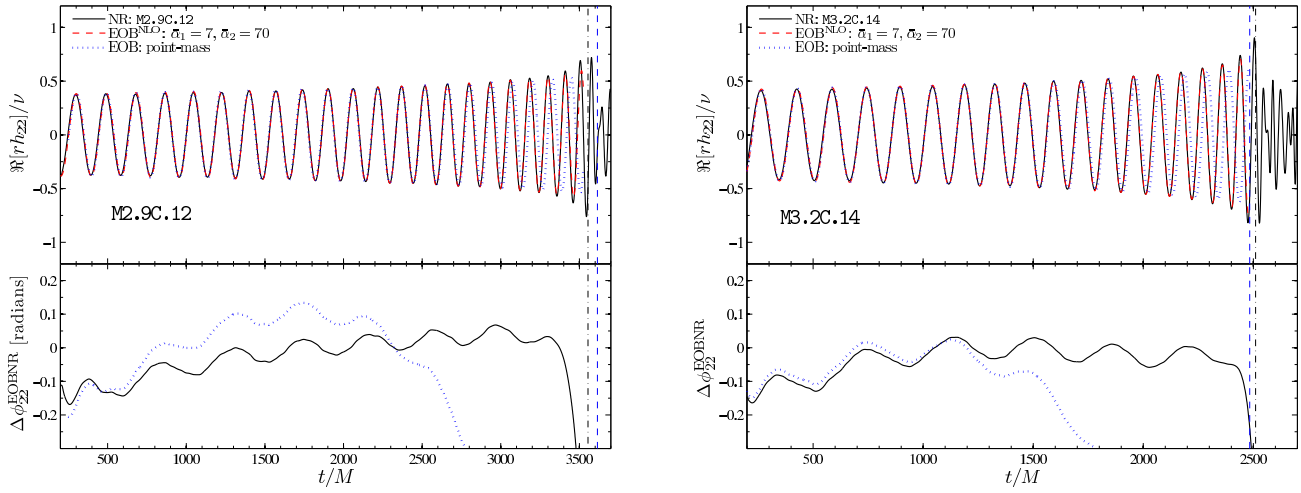

FIG. 3: Comparison between NR and AR phasing for the `M2.9C.12` (left panels) and `M3.2C.14` (right panels) binaries. The top panels show the real parts of the h_{22} waveforms, while the bottom panels show the corresponding phase differences. Note the excellent agreement almost up to the time of merger (vertical dashed and dot-dashed lines) and the very large errors when tidal effects are neglected (dotted line).

parameters in the NLO terms is made, the EOB model is able to reproduce all of the NR phase evolutions with great precision and essentially up to the merger. Typical errors over the $\gtrsim 20$ GW cycles are well within the error-bar of $\simeq \pm 0.24$ rad, thus leading to relative phase errors which are smaller than $\simeq 0.2\%$. Despite the degeneracy in the EOB modelling, the comparison with NR data has shown a clear *effective increase* of the Love numbers by a factor which is ≈ 2.5. Finally, we have also considered the differences between the NR waveforms and the ones obtained with Taylor-T4 PN expansion when tidal effects are introduced. Overall we have found that a good match with the NR data is possible also in this case, although with somewhat larger phasing errors. Most importantly however, the parameterization of the tidal effects is not the same for the two binaries considered and needs therefore to be suitably tuned in a case-by-case manner. This seems to suggest that the EOB-based representation of tidal effects may be more robust than the Taylor-T4 one.

The work reported here provides the first evidence that an accurate analytic modelling of the late inspiral of tidally interacting BNSs is possible, thereby opening the possibility to extract reliable information on the EOS of matter at nuclear densities from the data of the forthcoming advanced GW detectors. These encouraging results, however, also call for a continued synergy between more accurate numerical simulations and higher-order analytic results.

Acknowledgments. We thank the developers of `Cactus` and `Carpet` for their continuous improvements. The simulations were performed on Ranger (TACC/TG-MCA02N014) and Damiana (AEI). Partial support comes from the JSPS (19-07803 and

22740163) and from NASA (NNX09AI75G).

[1] N. Andersson, et al., Gen. Rel. Grav. *in press* arXiv:0912.0384.
[2] L. Baiotti, B. Giacomazzo, and L. Rezzolla, Phys. Rev. D **78**, 084033 (2008).
[3] T. Yamamoto, M. Shibata, and K. Taniguchi, Phys. Rev. D **78**, 064054 (2008); L. Baiotti, B. Giacomazzo, and L. Rezzolla, Class. Quantum Grav. **26**, 114005 (2009); L. Rezzolla, L. Baiotti, B. Giacomazzo, D. Link, and J.-A. Font, Class. Quantum Grav. **27**, 114105 (2010).
[4] M. Anderson, et al., Phys. Rev. Lett. **100**, 191101 (2008); Y. T. Liu, S. L. Shapiro, Z. B. Etienne, and K. Taniguchi, Phys. Rev. **D78**, 024012 (2008); B. Giacomazzo, L. Rezzolla, and L. Baiotti, MNRAS **399**, L164 (2009).
[5] J. S. Read, C. Markakis, M. Shibata, K. Uryu, J. D. E. Creighton, and J. L. Friedman, Phys. Rev. D **79**, 124033 (2009); K. Kiuchi, Y. Sekiguchi, M. Shibata, and K. Taniguchi, Phys. Rev. D **80**, 064037 (2009); K. Kiuchi, Y. Sekiguchi, M. Shibata, and K. Taniguchi, Phys. Rev. Lett. **104**, 141101 (2010).
[6] É. É. Flanagan and T. Hinderer, Phys. Rev. D **77**, 021502 (2008); T. Hinderer, Astrophys. J. **677**, 1216 (2008); T. Damour and A. Nagar, Phys. Rev. D **80**, 084035, 1 (2009); T. Binnington and E. Poisson, Phys. Rev. **D80**, 084018 (2009); T. Hinderer, B. D. Lackey, R. N. Lang, and J. S. Read, arXiv:0911.3535
[7] T. Damour and A. Nagar, Phys. Rev. D **81**, 084016 (2010).
[8] K. Uryu, F. Limousin, J. L. Friedman, E. Gourgoulhon, and M. Shibata, Phys. Rev. **D80**, 124004 (2009).
[9] A. Buonanno and T. Damour, Phys. Rev. D **59**, 084006 (1999); Phys. Rev. D **62**, 064015 (2000). T. Damour, Phys. Rev. D **64**, 124013 (2001).
[10] T. Damour and A. Nagar Phys. Rev. D **81**, 084016 (2009).
[11] A. Buonanno et al., Phys. Rev. **D79**, 124028 (2009).
[12] L. Baiotti et al., in preparation (2010).
[13] T. Damour and et al., Phys. Rev. D **77**, 084017 (2008).
[14] T. Damour and A. Nagar, Physical Review D **76**, 064028 (2007); Phys. Rev. **D77**, 024043 (2008).
[15] E. Schnetter, S. H. Hawley, and I. Hawke, Class. Quantum Grav. **21**, 1465 (2004); D. Pollney, C. Reisswig, et al., Phys. Rev. **D76**, 124002 (2007); L. Baiotti, et al., Phys. Rev. D **71**, 024035 (2005); B. Giacomazzo, and L. Rezzolla, Class. Quantum Grav. **24**, S235 (2007).
[16] E. Gourgoulhon, P. Grandclément, K. Taniguchi, J. A. Marck, and S. Bonazzola, Phys. Rev. D **63**, 064029 (2001).